Syntheses, structures, and electrochemical properties of four complexes based on 4-ferrocenylbutyrate ligand

Xiangru Meng, Wan Zhou, Yongfang Qi, Hongwei Hou *, Yaoting Fan

Department of Chemistry, Zhengzhou University, Henan 450052, PR China

ARTICLE INFO

ABSTRACT

Four ferrocenyl complexes with the formulas $\{[Mn(\eta^2\text{-}OOC(CH_2)_3Fc)_2(bbbm)]\cdot CH_3OH\}_n$ (**1**), $\{[Co(OOC(CH_2)_3Fc)(\eta^2\text{-}OOC(CH_2)_3Fc)(bbbm)]\cdot CH_3OH\}_n$ (**2**), $\{[Ni(OOC(CH_2)_3Fc)_2(bbbm)(CH_3OH)_2]\cdot 2CH_3OH\}_n$ (**3**) and $[Pb_6(\mu_2\text{-}OOC(CH_2)_3Fc)_2(\mu_3\text{-}OOC(CH_2)_3Fc)_2(\mu_2\text{-}\eta^2\text{-}OOC(CH_2)_3Fc)_2(\eta^2\text{-}OOC(CH_2)_3Fc)_2(\mu_4\text{-}O)_2]$ (**4**) (Fc = $(\eta^5\text{-}C_5H_5)Fe(\eta^5\text{-}C_5H_4)$, bbbm = 1,1-(1,4-butanediyl)bis-1H-benzimidazole) have been synthesized and characterized by single crystal X-ray diffraction. Owing to the different conformations of the bbbm units in complexes **1** (or **2**) and **3**, complexes **1** and **2** possess 1D helical chain structure with 2_1 screw axes along the *b*-direction, while complex **3** shows a 1D linear chain structure with ferrocenylbutyrate groups hanging on the chain. Complex **4** is a hexanuclear complex and exhibits a nano-scale wheel-like framework with six Pb(II) ions as a core and eight 4-ferrocenylbutyrate ligands as branches. The cyclic voltammetric studies show that the formal potentials of the four complexes are close to the free ferrocenylbutyrate ligand, which indicates that the coordination of the metal ions to the ferrocenyl ligand does not have significant effects on the redox potential of the ferrocenylbutyrate ligand. Further investigations suggest that the redox processes of the ferrocenylbutyrate ligand and complexes **1–4** are all chemically quasi-reversible processes and controlled by diffusion.

1. Introduction

The syntheses of the ferrocenyl derivatives and investigations of their properties have become an attractive research area since ferrocene was found in 1951. Due to the fascinating properties of the ferrocene moiety as well as the diversity of ferrocenyl derivatives, coordination chemists are interested in introducing ferrocene group into ligands in order to generate complexes possessing good electrochemical, magnetic and optical properties [1–6]. Furthermore, carboxylate group possesses strong coordinating capability and can display versatile coordination modes such as monodentate mode, symmetric bidentate mode, asymmetric bidentate mode, bridging mode, mix-bridging mode and so on [7–12]. Thus introducing ferrocenyl carboxylates into complexes and further exploiting the relationships between their structures and their properties have constituted one of the most attractive research fields in modern chemistry. Up to now, numerous complexes containing ferrocenyl carboxylates have been reported [13–16], whereas the complexes based on 4-ferrocenylbutyrate ligand are rarely reported [13]. Unlike other ferroceneyl carboxylates ligands, 4-ferrocenylbutyrate holds flexibility and can exhibit various

conformations and different coordination modes when it coordinates to metal ions. So it is a promising organometallic ligand to construct complexes.

On the other hand, flexible organic ligands can freely bend or rotate to meet the requirement of coordination geometries of metal ions in the assembly process [17–19]. And these advantages have been successfully exploited by many in recent times leading to a surge in intriguing architectures with the use of such ligands [20,21]. For example, the reactions of flexible neutral ligand methylenebis(3,5-dimethylpyrazole) with Zn(II) ion in the presence of various anions can lead to diverse structures, from discrete 0D structures to infinite 1D chains, 2D bilayer, and 3D metal–organic framework [21]. 1,1-(1,4-Butanediyl)bis-1H-benzimidazole (bbbm) is also a flexible linker and has been used to construct many complexes like $\{[Ni(bbbm)_2(H_2O)_2](NO_3)_2\cdot 2CH_3OH\cdot 6H_2O\}_n$, and $\{[Cd(bbbm)(SO_4)(H_2O)_2]CH_3OH\}_n$, and $[Pb(bbbm)_2(NO_3)_2]_n$ [22,23].

In order to enrich the categories and numbers of complexes with ferrocenyl carboxylates, in this paper, we select 4-ferrocenylbutyrate as the primary ligand and flexible organic ligand bbbm as subsidiary ligand. Through the assembly of the above ligands with Mn(II), Co(II), Ni(II), or Pb(II), two 1D helical chain complexes $\{[Mn(\eta^2\text{-}OOC(CH_2)_3Fc)_2(bbbm)]\cdot CH_3OH\}_n$ (**1**), $\{[Co(OOC(CH_2)_3Fc)(\eta^2\text{-}OOC(CH_2)_3Fc)(bbbm)]\cdot CH_3OH\}_n$ (**2**), one 1D linear chain complex $\{[Ni(OOC(CH_2)_3Fc)_2(bbbm)(CH_3OH)_2]\cdot 2CH_3OH\}_n$

* Corresponding author. Tel./fax: +86 371 67761744.
E-mail address: houhongw@zzu.edu.cn (H. Hou).

(**3**) and one scrollwheel-like hexanuclear complex [Pb$_6$(μ_2-OOC (CH$_2$)$_3$Fc)$_2$(μ_3-OOC(CH$_2$)$_3$Fc)$_2$(μ_2-η^2-OOC(CH$_2$)$_3$Fc)$_2$ (η^2-OOC(CH$_2$)$_3$ Fc)$_2$(μ_4-O)$_2$] (**4**) (Fc = (η^5-C$_5$H$_5$)Fe(η^5-C$_5$H$_4$)) have been synthesized and identified by X-ray diffraction analyses. In addition, the electrochemical properties of the ferrocenylbutyrate ligand and the four complexes have also been investigated through cyclic voltammetry (CV) method.

2. Experimental

2.1. Materials and methods

All chemicals were of reagent grade quality obtained from commercial sources and used without further purification. Carbon, hydrogen and nitrogen analyses were carried out on a FLASH EA 1112 elemental analyzer. IR data were recorded on a BRUKER TENSOR 27 spectrophotometer with KBr pellets in the 400–4000 cm^{-1} region.

2.2. Syntheses of sodium 4-ferrocenylbutyrate and 1,1-(1,4-butanediyl)bis-1H-benzimidazole

3-Ferrocenoylpropionic acid [24] and 4-ferrocenylbutyric acid [25] were prepared according to the literature methods. Sodium 4-ferrocenylbutyrate was obtained from the reaction of 4-ferrocenylbutyric acid with sodium methoxide in methanol. 1,1-(1,4-Butanediyl)bis-1H-benzimidazole (bbbm) was prepared according to the literature [26] except the modified purification procedure. The crude product was dissolved in a small amount of ethanol, and then the ethanol solution was added dropwise to a mass of distilled water by stirring. High purity products were separated as white acicular crystals and were isolated by filtration.

2.3. Synthesis of {[Mn(η^2-OOC(CH$_2$)$_3$Fc)$_2$(bbbm)]·CH$_3$OH}$_n$ (**1**)

A methanol solution (2 mL) of bbbm (0.02 mmol) was added dropwise to an aqueous solution (2 mL) of Mn(OAc)$_2$ (0.02 mmol). Fc(CH$_2$)$_3$COONa (0.04 mmol) in 4 mL of methanol was added dropwise to the above mixture. The resultant orange solution was allowed to stand at room temperature in the dark. Good quality

red crystals were obtained after about one month (Yield: 46%). Crystals of **1** are stable in the air. Anal. Calc. for C$_{47}$H$_{52}$Fe$_2$N$_4$O$_5$Mn: C, 61.39; H, 5.70; N, 6.09. Found: C, 61.33; H, 5.65; N, 5.98%. IR (cm^{-1}, KBr): 3360 m, 3089 s, 2936 s, 1552 s, 1504 m, 1457 m, 1416 s, 1293 m, 1253 m, 1198 m, 1103 m, 1040 m, 1004 m, 906 m, 820 m, 747 s, 640 m, 490 s.

2.4. Synthesis of {[Co(OOC(CH$_2$)$_3$Fc)(η^2-OOC(CH$_2$)$_3$Fc) (bbbm)]·CH$_3$OH}$_n$ (**2**)

The procedure was similar to that of **1** except that Co(OAc)$_2$·4H$_2$O was used instead of Mn(OAc)$_2$. Good quality purple crystals were obtained (Yield: 65%). Crystals of **2** are stable in the air. Anal. Calc. for C$_{47}$H$_{52}$Fe$_2$N$_4$O$_5$Co: C, 61.12; H, 5.68; N, 6.07. Found: C, 61.01; H, 5.85; N, 5.96%. IR (cm^{-1}, KBr): 3428 s, 3091 m, 2932 s, 1574 s, 1508 s, 1457 m, 1395 s, 1295 m, 1253 m, 1195 m, 1103 m, 1038 m, 1006 m, 916 w, 817 m, 749 s, 644 m, 493 s.

2.5. Synthesis of {[Ni(OOC(CH$_2$)$_3$Fc)$_2$(bbbm)(CH$_3$OH)$_2$]·2CH$_3$OH}$_n$ (**3**)

The procedure was similar to that of **1** except that Ni(OAc)$_2$·4H$_2$O was used instead of Mn(OAc)$_2$. Good quality orange crystals were obtained (Yield: 48%). Crystals of **3** are stable in the air. Anal. Calc. for C$_{50}$H$_{64}$Fe$_2$N$_4$O$_8$Ni: C, 58.91; H, 6.33; N, 5.50. Found: C, 58.64; H, 6.28; N, 5.61%. IR (cm^{-1}, KBr): 3426 s, 3096 s, 2937 s, 1603 s, 1550 s, 1511 s, 1458 s, 1409 s, 1297 m, 1263 m, 1198 m, 1104 m, 1043 m, 1004 m, 911 w, 822 m, 746 s, 638 w, 494 s.

2.6. Synthesis of [Pb$_6$(μ_2-OOC(CH$_2$)$_3$Fc)$_2$(μ_3-OOC(CH$_2$)$_3$Fc)$_2$(μ_2-η^2-OOC(CH$_2$)$_3$Fc)$_2$ (η^2-OOC(CH$_2$)$_3$Fc)$_2$(μ_4-O)$_2$] (**4**)

The procedure was similar to that of **1** except that Pb(NO$_3$)$_2$ was used instead of Mn(OAc)$_2$. Good quality orange crystals were obtained (Yield: 56%). But it is different from **1**, **2** and **3**, the bbbm ligand does not coordinate to Pb(II). If we change the reactants, only use Fc(CH$_2$)$_3$COONa to react with Pb(NO$_3$)$_2$, the same orange product was obtained. Crystals of **4** are stable in the air. Anal. Calc. for C$_{56}$H$_{60}$Fe$_4$O$_9$Pb$_3$: C, 39.06; H, 3.51. Found: C, 38.91; H, 3.55%. IR

Table 1
Crystal data and structure refinement for complexes 1–4.

Complexes	1	2	3	4
Formula	C$_{47}$H$_{52}$Fe$_2$N$_4$O$_5$Mn	C$_{47}$H$_{52}$Fe$_2$N$_4$O$_5$Co	C$_{50}$H$_{64}$Fe$_2$N$_4$O$_8$Ni	C$_{56}$H$_{60}$Fe$_4$O$_9$Pb$_3$
M$_r$	919.57	923.56	1019.46	1722.01
Crystal system	Orthorhombic	Orthorhombic	Triclinic	Triclinic
Space group	P2(1)2(1)2(1)	P2(1)2(1)2(1)	P$\bar{1}$	P$\bar{1}$
a (Å)	8.9090(18)	8.8966(18)	8.9085(18)	9.758(2)
b (Å)	17.101(3)	17.030(3)	9.854(2)	17.123(3)
c (Å)	28.547(6)	28.270(6)	13.963(3)	17.160(3)
α (°)	90	90	85.71(3)	96.88(3)
β (°)	90	90	80.14(3)	104.24(3)
γ (°)	90	90	86.56(3)	100.64(3)
V (Å^3)	4349.2(15)	4283.2(15)	1202.8(4)	2689.8(9)
Z	4	4	2	2
D$_c$ (g/cm^3)	1.404	1.432	1.407	2.126
μ (mm^{-1})	0.995	1.102	1.039	10.457
Reflns collected	47 797	47 348	14 635	32 983
Unique reflns	8524	8404	5495	12 328
R$_{int}$	0.0601	0.0987	0.0244	0.0309
Data/restraints/parameters	8524/0/535	8404/0/535	5495/0/301	12 328/0/649
GOF	1.081	1.061	1.094	1.031
R$_1$ [I > 2σ(I)]	0.0679	0.0870	0.0427	0.0387
wR$_2$ [I > 2σ(I)]	0.1492	0.1628	0.0934	0.0933
R$_1$[a] [all data]	0.0834	0.1240	0.0538	0.0496
wR$_2$[b] [all data]	0.1584	0.1825	0.1003	0.1034

[a] $R_1 = ||F_o| - |F_c||/|F_o|$.
[b] $wR_2 = [w(|F_o^2| - |F_c^2|)^2/w|F_o^2|^2]^{1/2}$. $w = 1/[\sigma^2(F_o^2) + 0.0297P^2 + 27.5680P]$, where $P = (F_o^2 + 2F_c^2)/3$.

(cm^{-1}, KBr): 3422 s, 3090 s, 2944 s, 1545 s, 1402 s, 1500 m, 1458 m, 1402 s, 1294 m, 1196w, 1104 m, 1031 m, 1004 m, 896 w, 815 s, 748 s, 638 w, 488 s.

2.7. Crystal structure determination

The data of the four complexes were collected on a Rigaku Saturn 724 CCD diffractomer (Mo Kα, λ = 0.71073 Å) at temperature of 20 ± 1 °C. Absorption corrections were applied by using multi-scan program. The data were corrected for Lorentz and polarization effects. The structures were solved by direct methods and refined with a full-matrix least-squares technique based on F^2 with the SHELXL-97 crystallographic software package [27]. All of the non-hydrogen atoms were refined anisotropically. The hydrogen atoms were assigned with common isotropic displacement factors and included in the final refinement by using geometrical restrains.

Table 2
Selected bond lengths (Å) and bond angles (°) for complexes **1–4**.

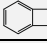|					
Complex 1[a]					
Mn(1)–O(4)	2.150(4)	Mn(1)–N(4)#1	2.188(4)	Mn(1)–N(1)	2.209(4)
Mn(1)–O(2)	2.226(5)	Mn(1)–O(1)	2.254(4)	Mn(1)–O(3)	2.440(5)
O(4)–Mn(1)–N(4)#1	103.78(18)	O(4)–Mn(1)–N(1)	91.91(16)	N(4)#1–Mn(1)–N(1)	100.57(16)
O(4)–Mn(1)–O(2)	155.7(2)	N(4)#1–Mn(1)–O(2)	87.43(18)	N(1)–Mn(1)–O(2)	107.3(2)
O(4)–Mn(1)–O(1)	109.41(19)	N(4)#1–Mn(1)–O(1)	144.46(18)	N(1)–Mn(1)–O(1)	90.81(17)
O(2)–Mn(1)–O(1)	57.03(17)	O(4)–Mn(1)–O(3)	55.86(16)	N(4)#1–Mn(1)–O(3)	94.53(17)
N(1)–Mn(1)–O(3)	147.02(16)	O(2)–Mn(1)–O(3)	102.4(2)	O(1)–Mn(1)–O(3)	93.69(18
Complex 2[b]					
Co(1)-O(3)	1.987(5)	Co(1)-N(1)	2.063(6)	Co(1)–N(4)#1	2.062(6)
Co(1)-O(2)	2.117(8)	Co(1)-O(1)	2.279(9)		
O(3)–Co(1)–N(1)	106.8(2)	O(3)–Co(1)–N(4)#1	99.3(2)	N(1)–Co(1)–N(4)#1	104.9(2)
O(3)–Co(1)–O(2)	149.0(3)	N(1)–Co(1)–O(2)	89.6(3)	N(4)#1–Co(1)–O(2)	101.6(3)
O(3)–Co(1)–O(1)	101.7(3)	N(1)–Co(1)–O(1)	143.4(3)	N(4)#1–Co(1)–O(1)	92.4(3)
O(2)–Co(1)–O(1)	55.0(3)				
Complex 3[c]					
Ni(1)–O(1)#1	2.0497(15)	Ni(1)–O(1)	2.0497(15)	Ni(1)–O(3)	2.0847(18)
Ni(1)–O(3)#1	2.0847(18)	Ni(1)–N(1)#1	2.1313(18)	Ni(1)–N(1)	2.1313(18)
O(1)#1–Ni(1)–O(1)	180.000(1)	O(1)#1–Ni(1)–O(3)	90.66(7)	O(1)–Ni(1)–O(3)	89.34(7)
O(1)#1–Ni(1)–O(3)#1	89.34(7)	O(1)–Ni(1)–O(3)#1	90.66(7)	O(3)–Ni(1)–O(3)#1	180.00(10)
O(1)#1–Ni(1)–N(1)#1	87.73(7)	O(1)–Ni(1)–N(1)#1	92.27(7)	O(3)–Ni(1)–N(1)#1	86.28(8)
O(3)#1–Ni(1)–N(1)#1	93.72(8)	O(1)#1–Ni(1)–N(1)	92.27(7)	O(1)–Ni(1)–N(1)	87.73(7)
O(3)–Ni(1)–N(1)	93.72(8)	O(3)#1–Ni(1)–N(1)	86.28(8)	N(1)#1–Ni(1)–N(1)	180.00(10)
Complex 4[d]					
Pb(1)–O(9)	2.221(4)	Pb(1)–O(2)	2.456(5)	Pb(1)–O(6)#1	2.573(5)
Pb(1)–O(1)	2.627(5)	Pb(1)–O(8)	2.657(5)	Pb(2)–O(9)#1	2.312(4)
Pb(2)–O(9)	2.329(4)	Pb(2)–O(4)	2.560(5)	Pb(2)–O(6)#1	2.601(5)
Pb(2)–O(3)	2.651(5)	Pb(3)–O(9)	2.349(4)	Pb(3)–O(7)	2.435(5)
Pb(3)–O(5)	2.474(5)	Pb(3)–O(4)	2.695(5)		
O(9)–Pb(1)–O(2)	81.99(16)	O(9)–Pb(1)–O(6)#1	73.44(14)	O(2)–Pb(1)–O(6)#1	73.83(16)
O(9)–Pb(1)–O(1)	80.75(15)	O(2)–Pb(1)–O(1)	50.92(14)	O(6)#1–Pb(1)–O(1)	121.53(16)
O(9)–Pb(1)–O(8)	78.14(14)	O(2)–Pb(1)–O(8)	119.17(16)	O(6)#1–Pb(1)–O(8)	146.68(16)
O(1)–Pb(1)–O(8)	69.31(16)	O(9)–Pb(1)–Pb(2)	37.95(10)	O(2)–Pb(1)–Pb(2)	54.35(11)
O(6)#1–Pb(1)–Pb(2)	45.63(11)	O(1)–Pb(1)–Pb(2)	83.07(11)	O(8)–Pb(1)–Pb(2)	114.06(11)
O(9)#1–Pb(2)–O(9)	76.61(14)	O(9)#1–Pb(2)–O(4)	105.37(15)	O(9)–Pb(2)–O(4)	74.94(15)
O(9)#1–Pb(2)–O(6)#1	81.65(16)	O(9)–Pb(2)–O(6)#1	71.25(14)	O(4)–Pb(2)–O(6)#1	142.77(16)
O(9)#1–Pb(2)–O(3)	77.61(15)	O(9)–Pb(2)–O(3)	108.11(15)	O(4)–Pb(2)–O(3)	50.25(16)
O(6)#1–Pb(2)–O(3)	158.69(16)	O(9)#1–Pb(2)–Pb(1)	96.60(10)	O(9)–Pb(2)–Pb(1)	35.90(9)
O(4)–Pb(2)–Pb(1)	97.81(12)	O(6)#1–Pb(2)–Pb(1)	45.01(11)	O(3)–Pb(2)–Pb(1)	142.42(11)
O(9)#1–Pb(2)–Pb(2)#1	38.48(9)	O(9)–Pb(2)–Pb(2)#1	38.14(9)	O(4)–Pb(2)–Pb(2)#1	90.12(12)
O(6)#1–Pb(2)–Pb(2)#1	72.67(11)	O(3)–Pb(2)–Pb(2)#1	93.58(12)	Pb(1)–Pb(2)–Pb(2)#1	63.57(2)
O(9)–Pb(3)–O(7)	75.55(14)	O(9)–Pb(3)–O(5)	108.58(15)	O(7)–Pb(3)–O(5)	81.48(17)
O(9)–Pb(3)–O(4)	72.06(14)	O(7)–Pb(3)–O(4)	137.10(15)	O(5)–Pb(3)–O(4)	82.97(17)

[a] Symmetry transformations used to generate equivalent atoms in **1**: #1 –x, y + 1/2, –z + 1/2.
[b] Symmetry transformations used to generate equivalent atoms in **2**: #1 –x + 2, y – 1/2, –z + 1/2.
[c] Symmetry transformations used to generate equivalent atoms in **3**: #1 –x + 1, –y + 2, –z + 1.
[d] Symmetry transformations used to generate equivalent atoms in **4**: #1 –x + 2, –y + 2, –z + 1.

Table 3
Main IR frequencies of complexes **1–4** (cm^{-1}).

Complexes	vO–H	Cp–H or Ar–H	CH$_2$	Cp–	⬡	Fe–Cp	v_a(COO)	v_s(COO)	Δ[a]	Structure
1	3360	3089	2936	1004	747	490	1504	1457	47	Bidentate
2	3428	3091	2933	1006	749	493	1574	1395	179	Unidentate
							1508	1457	51	Bidentate
3	3426	3096	2937	1004	747	494	1603	1409	194	Unidentate
4	3422	3090	2944	1004		488	1545	1402	143	Bridging
							1500	1458	42	Bidentate

[a] Δ is the separations between v_a(COO) and v_s(COO).

Crystallographic crystal data and structure processing parameters for complexes **1–4** are summarized in detail in Table 1. Selected bond lengths and bond angles are listed in Table 2.

2.8. Electrochemistry properties determination

The electrochemistry properties were determined by a CHI660B electrochemical analyzer utilizing the three-electrode configuration of a Pt working electrode, a Pt auxiliary electrode, and a saturated Ag/AgCl electrode as the reference electrode. The measurements were carried out in DMF solutions with 0.1 mol·dm^{-3} tetrabutylammonium perchlorate (TBAP) as a supporting electrolyte. Pure N_2 gas was bubbled through the electrolytic solution to remove oxygen.

3. Results and discussion

3.1. IR spectroscopy

The main IR frequencies of complexes **1–4** and the band assignments are listed in Table 3. The separations (Δ) between $v_a(COO)$ and $v_s(COO)$ are different for the unidentate, chelating (bidentate) and bridging complexes. In complex **1**, 4-ferrocenylbutyrate ligands exhibit the $v_a(COO)$ and $v_s(COO)$ at 1504 and 1457 cm^{-1} ($\Delta = 47$ cm^{-1}). This Δ value is comparable to those of bidentate complexes and 4-ferrocenylbutyrate ligands can be assigned to bidentate coordination mode [28]. In complex **2**, unidentate and bidentate 4-ferrocenylbutyrate ligands are mixed; the unidentate ligand exhibits the $v_a(COO)$ and $v_s(COO)$ at 1574 and 1395 cm^{-1} ($\Delta = 179$ cm^{-1}), whereas the bidentate ligand exhibits the $v_a(COO)$ and $v_s(COO)$ at 1508 and 1457 cm^{-1} ($\Delta = 51$ cm^{-1}). In complex **3**, 4-ferrocenylbutyrate ligands exhibit the $v_a(COO)$ and $v_s(COO)$ at 1603 and 1409 cm^{-1}, respectively ($\Delta = 194$ cm^{-1}). Thus, 4-ferrocenylbu-
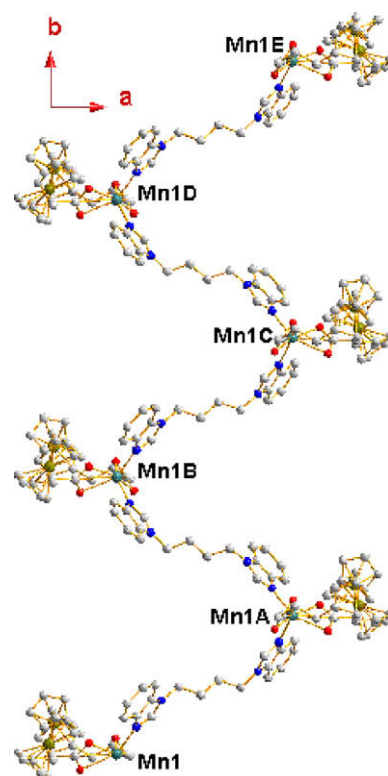

Fig. 1b. ORTEP drawing of 1D helical chain structure of complex **1** (H atoms and uncoordinated solvent molecules are omitted for clarity).

tyrate ligands in complex **3** are concluded to be unidentate coordination mode. The coordination modes of 4-ferrocenylbutyrate
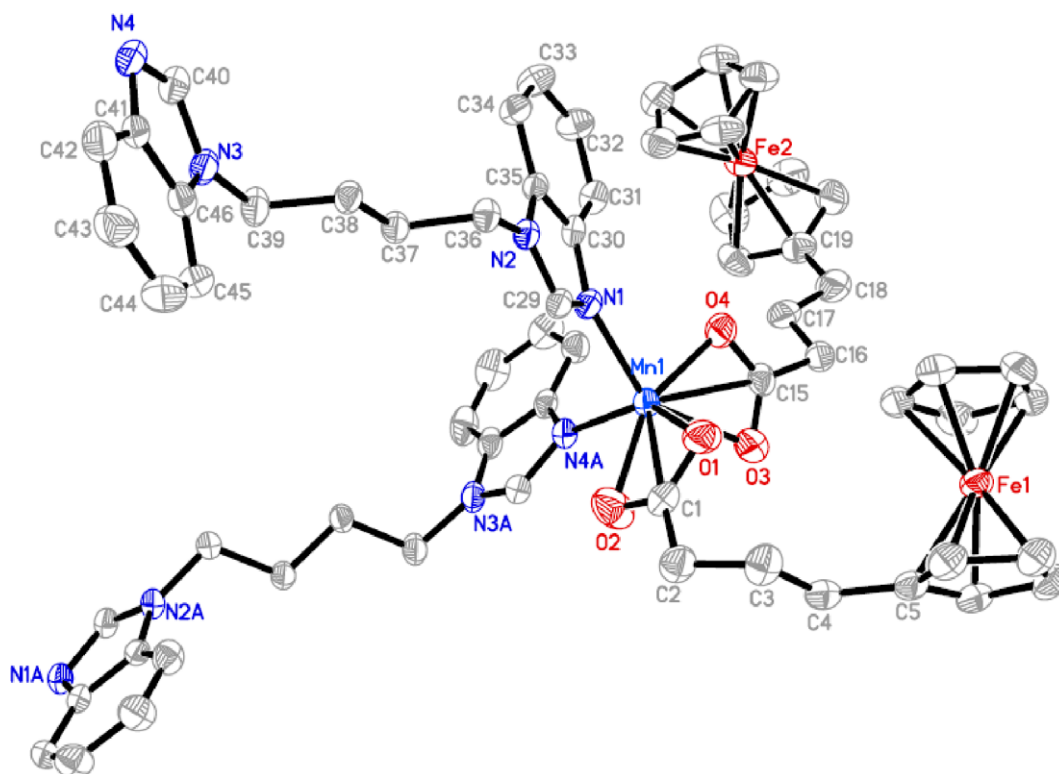

Fig. 1a. The coordination environment of Mn(II) ion in complex **1** with atom numberings, showing 30% thermal ellipsoïds. Hydrogen atoms and solvent molecule are omitted for clarity.
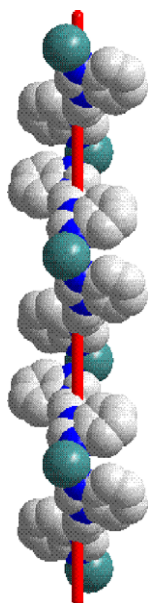
Fig. 1c. Space-filling model of helical chains of complex **1** (H atoms, uncoordinated solvent molecules and ferrocenylbutyrate groups are omitted for clarity).

ligands in complex **4** are complicated. The separations (Δ) between $v_a(COO)$ and $v_s(COO)$ are 143 and 42, respectively. Therefore, the 4-ferrocenylbutyrate ligands in complex **4** coordinate to the central metal ions with bridging and chelating modes. The above analyses are confirmed by the results of the X-ray diffraction.

3.2. Crystal structure of {[Mn(η^2-OOC(CH$_2$)$_3$Fc)$_2$(bbbm)]·CH$_3$OH}$_n$ (**1**)

Single crystal X-ray diffraction analysis reveals that complex **1** crystallizes in a space group $P2_12_12_1$ and has 1D helical chain

structure. As shown in Fig. 1a, each six-coordinate Mn(II) center is in a seriously distorted octahedral geometry, defined by two nitrogen atoms from two bbbm units and four oxygen atoms from two carboxyl groups with asymmetric bidentate fashion. Atoms O1, O2, O4, N4A and Mn1 form the equatorial plane, while atoms O3 and N1 occupy the axial positions. The bond angle of O3–Mn1–N1 is 147.02(16)°. The Mn–O distances range from 2.150(4) to 2.440(5) Å, and the Mn–N distances are 2.188(4) and 2.209(4) Å, respectively. These Mn–O and Mn–N bond lengths are close to those in the related Mn(II) complexes like {[Mn(μ_2-OOCH$_4$C$_6$Fc)$_2$(phen)]$_n$ [29] and [Mn$_{13}$O$_8$(OCH$_3$)$_6${Fc(CO$_2$)$_2$}$_6$]·8H$_2$O·2CH$_3$OH·2(CH$_3$)$_2$CO [30].

In the crystal structure of complex **1**, there are two crystallographically independent 4-ferrocenylbutyrate moieties. One kind of the 4-ferrocenylbutyrate moieties (Fe1) adopts the GT conformation and the cyclopentadienyl rings within the ferrocenyl group deviate by 2.8° from the eclipsed conformation. The other kind of the 4-ferrocenylbutyrate moieties (Fe2) adopts the TT conformation and the cyclopentadienyl rings within the ferrocenyl group deviate by 2.0° from the eclipsed conformation. But all of the bbbm moieties in **1** are equivalent and adopt the TTT conformation. Furthermore, As shown in Fig. 1b, the Mn(II) ions are linked by bbbm units leading to the infinite 1D chain. The intrachain Mn···Mn separation separated by bbbm is 13.897 Å. Notably the 1D chain structure is a helix with a pitch of 17.101(3) Å following a 2_1 screw axis along the b-direction (Fig. 1c). To the best of our knowledge, although a lot of helical structures have been reported, the helical chain structures containing ferrocenyl carboxylate groups are extremely rare.

3.3. Crystal structure of {[Co(OOC(CH$_2$)$_3$Fc)(η^2-OOC(CH$_2$)$_3$Fc)(bbbm)]·CH$_3$OH}$_n$ (**2**)

As depicted in Fig. 2a, the coordination number of Co(II) ion in complex **2** is different from that of Mn(II) ion in complex **1**. Each
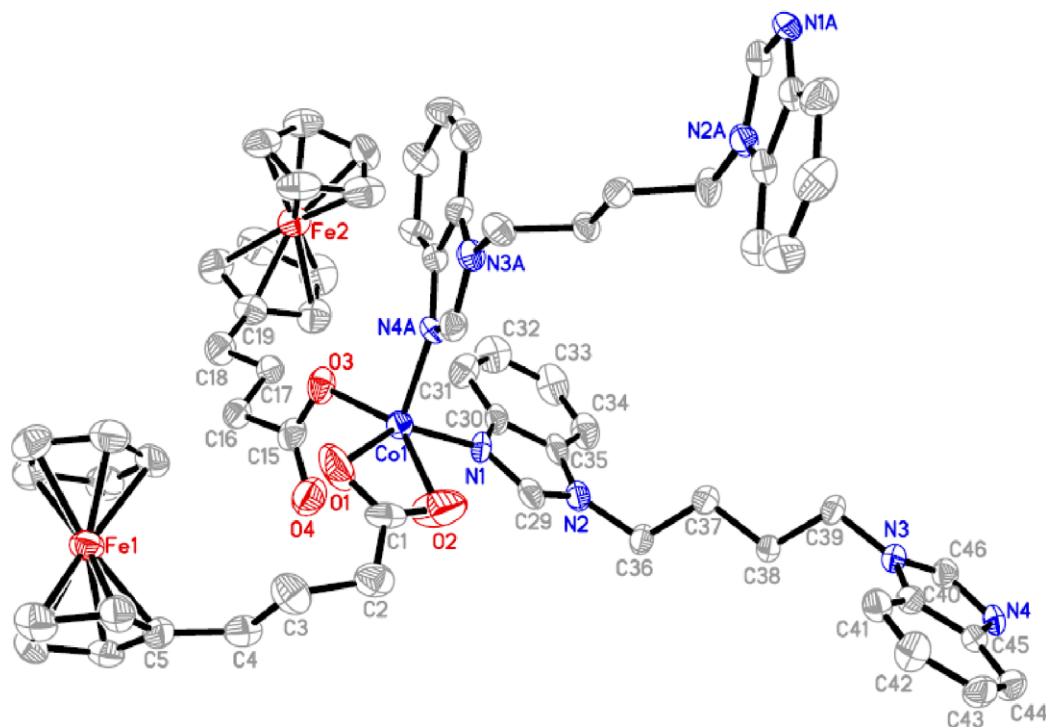

Fig. 2a. The coordination environment of Co (II) ion in complex **2** with atom numberings, showing 30% thermal ellipsoids. Hydrogen atoms and solvent molecule are omitted for clarity.
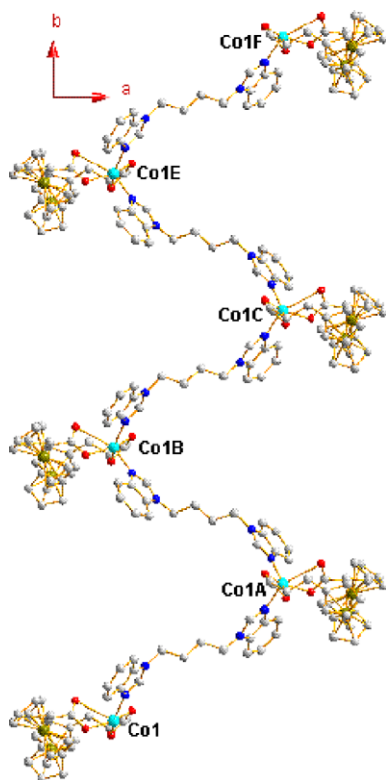
Fig. 2b. ORTEP drawing of 1D helical chain structure of complex **2** (H atoms and uncoordinated solvent molecules are omitted for clarity).
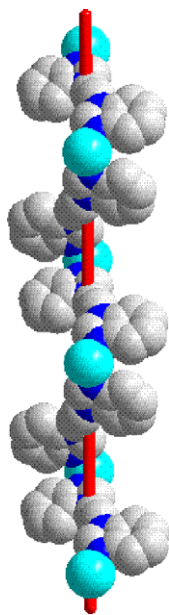

Fig. 2c. Space-filling model of helical chains of complex **2** (H atoms, uncoordinated solvent molecules and ferrocenylbutyrate groups are omitted for clarity).

Co(II) center is five coordinated by two nitrogen atoms from two bbbm groups and three oxygen atoms from two 4-ferrocenylbuty-rate moieties. The Co–O distances range from 1.987(5) to 2.279(9) Å and Co–N distances are 2.062(6) Å and 2.063(6) Å, respectively, which are close to the reported Co(II) complexes [31,32]. Atoms O1, O2, O3, N1 and Co1 form the equatorial plane. So the local environment around the central Co(II) ion can be best

described as a distorted tetra-pyramidal geometry. Similar to complex **1**, all of the bbbm units adopt the TTT conformation and the 4-ferrocenylbutyrate moieties exhibit GT and TT conformations. The cyclopentadienyl rings within the ferrocenyl group present the eclipsed conformation. The bbbm groups acting as organic linkers connect the $Co(OOC(CH_2)_3Fc)_2$ units forming the infinite 1D helix chain with the Co$\cdots$Co separation of 13.615 Å (Fig. 2b and c). The pitch of the helix chain is 17.030(3) Å along the b-direction.

3.4. Crystal structure of $\{[Ni(OOC(CH_2)_3Fc)_2(bbbm)(CH_3OH)_2]\cdot 2CH_3OH\}_n$ (**3**)
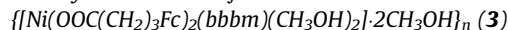
It is different from complexes **1** and **2**, complex **3** crystallizes in a space group $P\bar{1}$ and shows a 1D linear chain structure. All of the Ni(II) ions, the 4-ferrocenylbutyrate ligands, the bbbm groups and the coordinated methanol molecules are equivalent, respectively. Each Ni(II) center is six-coordinated and exhibits a slightly distorted octahedral environment supplied by four oxygen atoms from two terminal monodentate carboxylate groups and two coordinated methanol molecules and two nitrogen atoms from two bbbm groups, as illustrated in Fig. 3. Around the central Ni(II) ion, the bond lengths of Ni–O are 2.0847(18) (from methanol molecule) and 2.0497(15) Å (from carboxylate group) and the bond length of Ni–N is 2.1313(18) Å. The bond angles around the Ni(II) ion are close to 90° or 180°. In each ferrocenyl moiety, cyclopentadienyl rings are co-planar and nearly parallel with a dihedral angle of 0.8°. Cyclopentadienyl rings within the ferrocenyl group deviate by 7.2° from the eclipsed conformation which is larger than those in complexes **1** and **2**. Furthermore, the conformation of the bbbm groups in complex **3** is also different from those in complexes **1** and **2**, they adopt the GTG conformation and connect $[Ni(OOC(CH_2)_3Fc)_2(CH_3OH)_2]$ units leading to the 1D linear chain structure. All of the Ni(II) ions in one chain are in a straight line, and the intrachain Ni$\cdots$Ni separation across the bbbm linker is 12.881 Å. Along the 1D polymeric chain, all of the 4-ferrocenylbu-tyrate moieties with the monodentate syn-coordination mode of the carboxy groups adopt the same TG conformation and situate on the opposite sides of the central metal ion.

3.5. Crystal structure of $[Pb_6(\mu_2\text{-}OOC(CH_2)_3Fc)_2(\mu_3\text{-}OOC(CH_2)_3Fc)_2(\mu_2\text{-}\eta^2\text{-}OOC(CH_2)_3Fc)_2(\eta^2\text{-}OOC(CH_2)_3Fc)_2(\mu_4\text{-}O)_2]$ (**4**)

The X-ray diffraction analysis reveals that **4** is a hexanuclear complex and shows a wheel-like structure. As shown in Fig. 4a, there are three crystallographically independent Pb(II) ions and four crystallographically independent 4-ferrocenylbutyrate moieties. As depicted in Fig. 4b, Pb1 and Pb2 can be defined as penta-coordinated. Each Pb1 ion coordinates to five oxygen atoms, of which two from Fe1 moiety, one from Fe3A moiety, one from Fe4 moiety, and one from $\mu_4\text{-}O^{2-}$ anion leading to an extremely distorted penta-pyramidal geometry. For Pb2, the five oxygen atoms are from Fe2, Fe3A moieties and $\mu_4\text{-}O^{2-}$ anions resulting in an extremely distorted penta-pyramidal geometry. But the coordination number of Pb3 is four, of which one from Fe2 moiety, one from Fe3 moiety, one from Fe4 moiety, and one from $\mu_4\text{-}O^{2-}$ anion leading to a tetra-pyramidal geometry. In addition, in complex **4**, the six Pb(II) ions inhabit the six apexes of a presumed compressed Pb_6 octahedron and are bridged by two $\mu_4\text{-}O^{2-}$ anions from the inner of the Pb_6 octahedron core. Pb1, Pb1A, Pb3, and Pb3A form an equatorial plane with the Pb1–Pb1A and Pb3–Pb3A distances of 6.528 and 6.763 Å, respectively. Pb2 and Pb2A occupy the axial positions and the Pb2–Pb2A distance is 3.642 Å. As shown in Fig. 4b, although the four kinds of 4-ferrocenylbutyrate moieties all adopt the GT conformation, their coordination modes are different. They display bidentate coordination mode ($\eta^2\text{-}OOC(CH_2)_3Fc$), tridentate

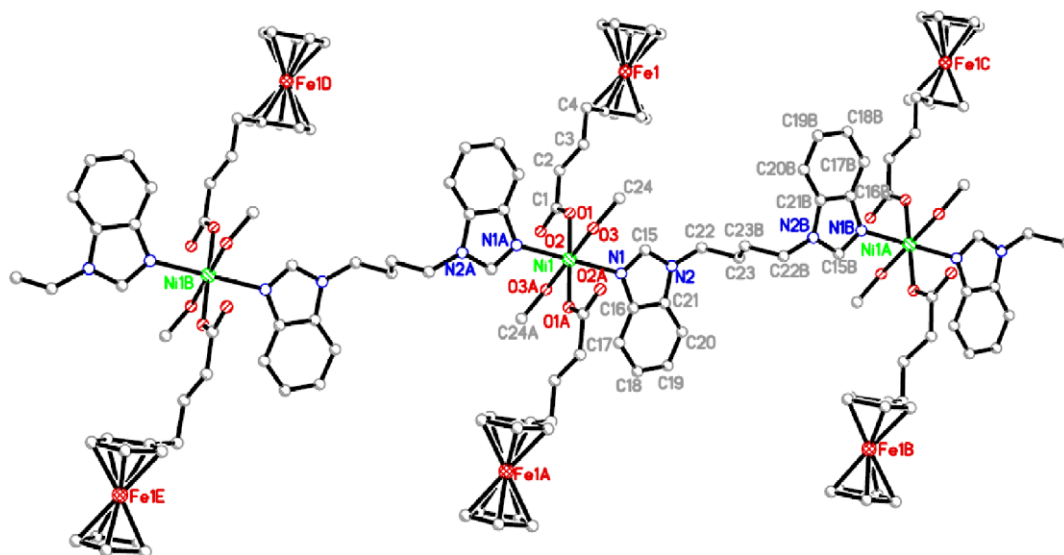**Fig. 3.** One-dimensional chain structure of complex **3**. Hydrogen atoms and solvent molecules are omitted for clarity.

coordination modes (μ_2-η^2-OOC(CH$_2$)$_3$Fc and μ_3-OOC(CH$_2$)$_3$Fc), and bridging coordination mode (μ_2-OOC(CH$_2$)$_3$Fc), respectively.

In addition, an interesting feature of the structure can be noticed from Fig. 4a that eight ferrocene fragments are arranged around the Pb$_6$ octahedron leading to a nano-scale wheel-like framework with 4-ferrocenylbutyrate units as branches, and the distance between the terminal hydrogen atoms (H27A and H27B) of the cyclopentadienyl rings at the inverse sides of the molecule is about 22.416 Å.

From the discussion above, it is clear that the composition and structure of complex **4** is different from those of **1**, **2** and **3**, in which central metal ions coordinate to both ferrocenyl carboxylates and bbbm ligands simultaneously. Furthermore, the ligands around the central metal ions of complexes **1**, **2** and **3** are holodirected, in which the bonds to ligand atoms are distributed throughout the surface of an encompassing globe. However in complex **4**, only ferrocenyl carboxylates coordinate to Pb(II) ion, and its structure is similar to other reported multinuclear lead(II) carboxylate and oxo clusters like [Pb$_6$O$_2$(OOCCH=CHFc)$_8$] and [Pb$_6$O$_2$-(C$_{14}$H$_9$O$_3$)$_8$] (C$_{14}$H$_9$O$_3$ = benzoylbenzoate) [15,33–35]. This imply that Pb(II) ion has strong capacity for binding with oxygen and can be easily coordinated by carboxylate ligands. This phenomenon can be explained by the particular coordination modes of Pb(II) ion. In complex **4**, the coordination numbers of the Pb(II) ions are relatively low (4 or 5); this is favorable to hemidirected, in which the bonds to ligand atoms are directed throughout only part of an encompassing globe due to the stereochemical activity of the lone pair of electrons. Furthermore, there is steric hindrance effect when the nitrogen atoms coordinate to Pb(II) ions since the nitrogen atoms are located in the benzimidazole ring. This also can cause bbbm not easily to coordinate to Pb(II) ion. Other reasons have yet to be further explored. So only ferrocenyl carboxylates coordinate to Pb(II) ion in complex **4**.

3.6. Electrochemical studies

In our previous studies, we have determined the number-average molecular weights (Mn) and weight-average molecular weights (Mw) of the coordination polymers based on ferrocenyl carboxylate derivatives and the results indicated that they were not dissociated in DMF solution [13,29]. Thus, we confirm that the skeletons of the four complexes are intact in DMF solution.

So the electrochemical experiments of these complexes in DMF solution can veritably represent the electrochemistry properties of them. Here we use the cyclic voltammetry (CV) method to study the electrochemical properties of free the 4-ferrocenylbutyrate ligand and complexes **1**–**4** in DMF solutions.

The electrochemical parameters obtained from the CV are summarized in Table 4. The cyclic voltammetric behaviors of the 4-ferrocenylbutyrate ligand and the four complexes all show one pair of well-defined and stable redox waves in the potential range of 0.0–1.0 V, which are attributed to the Fc/Fc$^+$ redox process. It is interesting to find that the formal potentials (E^0) of complexes **1**–**4** are all nearly identical to that of the 4-ferrocenylbutyrate ligand, which indicates that the coordination of metal ions to the ferrocenyl ligand does not have significant effects on the redox potential of the 4-ferrocenylbutyrate ligand. The electrochemical behaviors
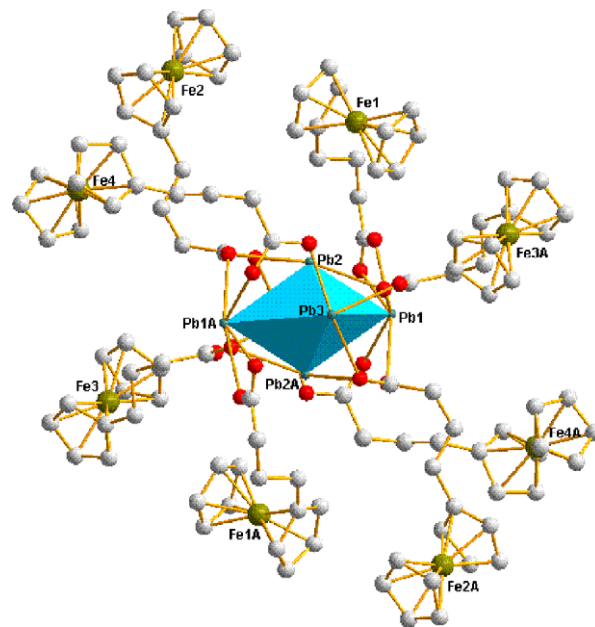

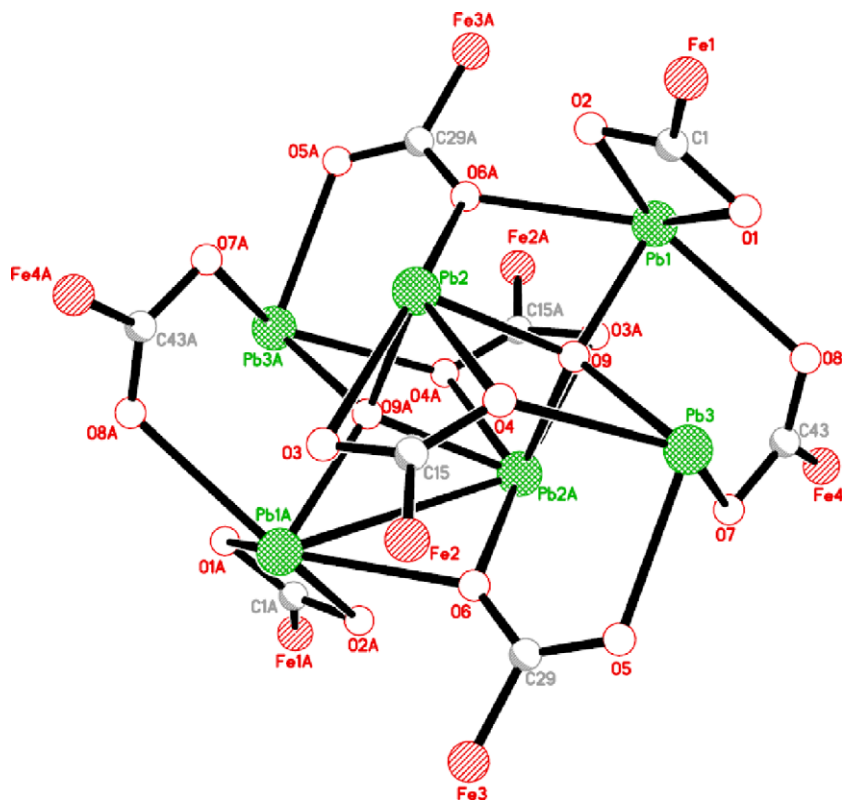**Fig. 4a.** The nano-scale wheel-like framework of complex **4**.

Fig. 4b. The coordination environment of Pb(II) ion and the coordination modes of 4-ferrocenylbutyrate moieties in complex **4** (H atoms are omitted for clarity, and Fe represents $(\eta^5\text{-}C_5H_5)Fe(\eta^5\text{-}C_5H_4)(CH_2)_3$-group.

of the complexes are analogous to that of the 4-ferrocenylbutyrate ligand.

If we keep the compositions of the test solution and change the scan rates (from 50 to 500 mV s^{-1}) in the potential range of 0.0–1.0 V, we can get the cyclic voltammetric diagrams of the 4-ferrocenylbutyrate ligand and complexes **1**–**4** at different scan rates. The results show that the oxidation wave potentials show gradual increase and the reduction wave potentials show gradual decrease as the scan rates increase; the anodic to cathodic peak current ratios (i_{pa}/i_{pc}) are close to 1. Judging from the above values, it was tentatively assigned that the redox processes of the 4-ferrocenylbutyrate ligand and complexes **1**–**4** are chemically quasi-reversible processes [36]. Additionally, as shown in Fig. 5, the dependence of the currents at different scan rates on the square root of the scan rates is linear. So the redox processes of the 4-ferrocenylbutyrate ligand and complexes **1**–**4** are all controlled by diffusion [37].
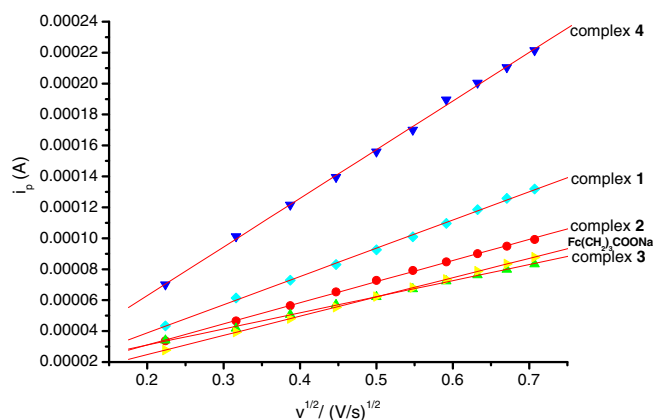

Fig. 5. Dependence of the currents on the square root of the scan rates.

Table 4
Electrochemical data of Fc(CH$_2$)$_3$COONa and complexes **1**–**4**.

Compounds	E_{pa} (V)[a]	E_{pc} (V)[a]	ΔE (mV)[b]	E^0 (V)[c]	i_{pa}/i_{pc}[d]
Fc(CH$_2$)$_3$COONa	0.554	0.473	81	0.514	1.02
1	0.549	0.461	88	0.505	1.05
2	0.564	0.478	86	0.521	1.10
3	0.561	0.479	82	0.520	1.05
4	0.557	0.448	109	0.503	1.10

All potentials are referred to Ag/AgCl in DMF solution, v = 100 mV/s.
[a] E_{pa} and E_{pc} are the oxidation and reduction wave potentials, respectively.
[b] $\Delta E = (E_{pa} - E_{pc})$.
[c] E^0 is the formal potential and $E^0 = (E_{pa} + E_{pc})/2$.
[d] i_{pa} and i_{pc} are the oxidation and reduction wave currents, respectively.

4. Conclusion

In this paper, four new complexes **1**–**4** were constructed by sodium 4-ferrocenylbutyrate and 1,1-(1,4-butanediyl)bis-1H-benzimidazole (bbbm) with the corresponding metal salts. Single crystal X-ray diffraction studies reveal that the different conformations of the bbbm units can result in substantial structural difference: the bbbm units adopt the TTT conformation in complexes **1** and **2** leading to the formation of the 1D helical chain structure, while in complex **3** the bbbm units adopt the GTG conformation resulting in the formation of the 1D linear chain structure. Complex **4** is a hexanuclear complex with a nano-scale wheel-like structure. Further investigations reveal that the electrochemical

properties of the four complexes are close to those the free ferrocenylbutyrate ligand. This indicates that the coordination of the metal ions to the ferrocenyl ligand does not have significant effects on electrochemical properties of the ferrocenylbutyrate ligand.

Acknowledgments

Appendix A. Supplementary data

CCDC 743247, 743248, 743249, 743250 contains the supplementary crystallographic data for this paper. These data can be obtained free of charge from The Cambridge Crystallographic Data Centre via http://www.ccdc.cam.ac.uk/data_request/cif. Supplementary data associated with this article can be found, in the online version, at doi:10.1016/j.jorganchem.2009.12.015.

References

[1] Z. Zeng, A.A.J. Torriero, M.J. Belousoff, A.M. Bond, Chem. Eur. J. 15 (2009) 10988–10996.
[2] H.R. Shahsavari, M. Rashidi, S.M. Nabavizadeh, S. Habibzadeh, F.W. Heinemann, Eur. J. Inorg. Chem. 25 (2009) 3814–3820.
[3] C.D. Varnado, V.M. Lynch, C.W. Bielawski, Dalton Trans. (2009) 7253–7261.
[4] H.W. Hou, L.K. Li, G. Li, Y.T. Fan, Y. Zhu, Inorg. Chem. 42 (2003) 3501–3508.
[5] S. Santi, C. Durante, A. Donoli, A. Bisello, L. Orian, A. Ceccon, L. Crociani, F. Benetollo, Organometallics 28 (2009) 3319–3326.
[6] Y. Fan, I.P.C. Liu, P.E. Fanwick, T. Ren, Organometallics 28 (2009) 3959–3962.
[7] Y. Liu, H. Hou, Q. Chen, Y. Fan, Cryst. Growth Des. 8 (2008) 1435–1442.
[8] H. Arora, F. Lloret, R. Mukherjee, Dalton Trans. (2009) 9759–9769.
[9] J. Hunger, H. Krautscheid, J. Sieler, Cryst. Growth Des. 9 (2009) 4613–4625.
[10] R. Horikoshi, K. Okazawa, T. Mochida, J. Organomet. Chem. 690 (2005) 1793–1799.
[11] C. Yenikaya, M. Poyraz, M. Sari, F. Demirci, H. Ilkimen, O. Bueyuekguengoer, Polyhedron 28 (2009) 3526–3532.
[12] M.A.S. Aquino, I.W. Wyman, Trends Inorg. Chem. 8 (2004) 1–21.
[13] E. Zhang, H. Hou, X. Meng, Y. Liu, Y. Liu, Y. Fan, Cryst. Growth Des. 9 (2009) 903–913.
[14] V. Mereacre, D. Prodius, A.M. Ako, S. Shova, C. Turta, K. Wurst, P. Jaitner, A.K. Powell, Polyhedron 28 (2009) 3551–3555.
[15] L.K. Li, Y.L. Song, H.W. Hou, Y.T. Fan, Y. Zhu, Eur. J. Inorg. Chem. (2005) 3238–3249.
[16] J. Kuehnert, T. Rueffer, P. Ecorchard, B. Braeuer, Y. Lan, A.K. Powell, H. Lang, Dalton Trans. (2009) 4499–4508.
[17] R. Bronisz, Eur. J. Inorg. Chem. (2004) 3688–3695.
[18] U. García-Couceiro, O. Castillo, A. Luque, J.P. García-Terán, G. Beobide, P. Román, Cryst. Growth Des. 6 (2006) 1839–1847.
[19] R. Bronisz, Inorg. Chim. Acta 357 (2004) 396–404.
[20] C. Deissler, F. Rominger, D. Kunz, Dalton Trans. (2009) 7152–7167.
[21] R. Mondal, T. Basu, D. Sadhukhan, T. Chattopadhyay, M.K. Bhunia, Cryst. Growth Des. 9 (2009) 1095–1105.
[22] X. Meng, Y. Song, H. Hou, Y. Fan, G. Li, Y. Zhu, Inorg. Chem. 42 (2003) 1306–1315.
[23] Q. Chang, X. Meng, Y. Song, H. Hou, Inorg. Chim. Acta 358 (2005) 2117–2124.
[24] K.L. Rinehart, R.J. Curby, P.E. Sokol, J. Am. Chem. Soc. 79 (1957) 3420–3424.
[25] P. Wang, X. Jing, C. Mei, X. Xiao, G. Zhu, Huaxue Shiji (Chin. Ed.) 22 (2000) 196–197.
[26] X.J. Xie, L. Cheng, A.H. Zheng, Y.L. Yang, Hecheng Huaxue (Chin. Ed.) 8 (2000) 252–255.
[27] G.M. Sheldrick, SHELXL-97 Program for Refining Crystal Structure Refinement, University of Göttingen, Germany, 1997.
[28] K. Nakamoto, Infrared and Raman Spectra of Inorganic and Coordination Compounds, Part B, sixth ed., John Wiley & Sons, Inc., Hoboken, New Jersey, 2009. pp. 64–67.
[29] H.W. Hou, L.K. Li, Y. Zhu, Y.T. Fan, Y.Q. Qiao, Inorg. Chem. 43 (2004) 4767–4774.
[30] M. Kondo, R. Shinagawa, M. Miyazawa, M.K. Kabir, Y. Irie, T. Horiba, T. Naito, K. Maeda, S. Utsuno, F. Uchida, Dalton Trans. (2003) 515–516.
[31] S.S. Massoud, K.T. Broussard, F.A. Mautner, R. Vicente, M.K. Saha, I. Bernal, Inorg. Chim. Acta 361 (2008) 123–131.
[32] R. Herchel, R. Boča, Dalton Trans. (2005) 1352–1353.
[33] M.R.S.J. Foreman, M.J. Plater, J.M.S. Skakle, J. Chem. Soc., Dalton Trans. (2001) 1897–1903.
[34] A. Thirumurugan, R.A. Sanguramath, C.N.R. Rao, Inorg. Chem. 47 (2008) 823–831.
[35] P. Nockemann, B. Thijs, K.V. Hecke, L.V. Meervelt, K. Binnemans, Cryst. Growth Des. 8 (2008) 1353–1363.
[36] Y. Xu, F. Wang, Y. Fu, Q.H. Zhang, B.X. Ye, M.P. Song, Y.J. Wu, Chem. J. Chin. Univ. 26 (2005) 1081–1085.
[37] Y.L. Ma, Chem. Res. Appl. 16 (2004) 551–552.